LAWRENCE
LIVERMORE
NATIONAL
LABORATORY

LLNL-JRNL-615497

Ground-state and isomeric-state cross section for 181Ta(n,2n)180Ta between 8 and 15 MeV

A. P. Tonchev, C. Bhatia, M. Gooden, W. Tornow

February 4, 2013

Phys. Rev. C

Disclaimer

Ground-state and isomeric-state cross section for ^{181}Ta($n,2n$)^{180}Ta between 8 and 15 MeV

C. Bhatia,[1,2*] M.E. Gooden,[2,3] W. Tornow, [1,2] A.P. Tonchev[4]

[1]*Department of Physics, Duke University, Durham, North Carolina 27708, USA*
[2]*Triangle Universities Nuclear Laboratory, Durham, North Carolina 27708, USA*
[3]*Department of Physics, North Carolina State University, Raleigh, North Carolina 27695, USA*
[4]*Physics Division, Lawrence Livermore National Laboratory, Livermore, California 94550, USA*
chitra@tunl.duke.edu

Using the activation technique, the cross section for the reaction ^{181}Ta($n,2n$)^{180g}Ta was measured from 8 to 15 MeV in small energy steps to resolve inconsistencies in the existing database. The 93.4 keV γ ray from the decay of the ^{180g}Ta ground state was recorded with a HPGe detector. The monitor reactions ^{27}Al(n,α)^{24}Na and ^{197}Au($n,2n$)^{196}Au were used for neutron fluence determination. The ENDF VII.1 and TENDL 2011 evaluations are in considerable disagreement with the present data, which in turn agree very well with the majority of the existing data in the 14 MeV energy region. A detailed analysis using the code TALYS was performed to describe the present data and to predict the ($n,2n$) cross section to the isomeric state of ^{180}Ta.

PACS number(s): 24.60.Dr, 25.40.Fq, 25.45.−z, 24.10.−i.

I. INTRODUCTION

Tantalum plays an important role in nuclear fission and fusion applications. For example, tantalum was used in the past as witness foils (chemical tracers) in underground tests of nuclear devices to assess their performance by recording the yield of the reaction ^{181}Ta($n,2n$)^{180g}Ta. More recently, in the design of accelerator driven systems, tantalum has been considered as the material of choice for the spallation target. Very recently, the ^{181}Ta($n,2n$)^{180g}Ta reaction is being viewed as an important diagnostic tool for studying and understanding the thermonuclear burn in the deuterium-tritium fuel capsule used in inertial confinement fusion research at the National Ignition Facility (NIF) at Livermore National Laboratory. In addition, the isotope ^{180}Ta, often called the rarest isotope in the universe, has been subject of many fundamental physics studies due to the fact that it exists naturally only in its isomeric state. For the most part, this nucleus is bypassed by the major nucleosynthesis mechanisms of the *s*- and *r*- processes. That is the reason why

*Present address: Medical Physics and Applied Radiation Sciences, McMaster University, 1280 Main Street West, General Sciences Building, Hamilton, ON *L8S 4K1*, Canada.

this isotope has the lowest abundance of any stable nuclides. The reaction mechanisms leading to the isomeric or ground state of ^{180}Ta are of paramount importance for the understanding of the production of ^{180m}Ta.

Unfortunately, the existing data for the ^{181}Ta($n,2n$)^{180g}Ta reaction cross section are inconsistent. In the well-studied energy region around 14 MeV, the data can be grouped into two bands which differ by about 60%, as can be seen from Fig. 1, which also shows that the ENDF VII.1 [1] and TENDL 2011 [2] evaluations favor the upper band. In view of this unsatisfactory situation and to provide more data below 12 MeV and closer to threshold than currently available, a new attempt was made to provide a definitive data set for the ^{181}Ta($n,2n$)^{180g}Ta reaction cross section in the 8 to 15 MeV energy range. This energy range is of special interest for applications as well as for nuclear astrophysics studies, and theoretical approaches aimed at calculating the ^{181}Ta($n,2n$)^{180m}Ta and ^{181}Ta($n,2n$)^{180g}Ta cross section at energies higher than studied in the present work.

II. EXPERIMENTAL PROCEDURE

The threshold energy for initiating the reaction ^{181}Ta($n,2n$)^{180g}Ta is 7.62 MeV. The ^{2}H(d,n)^{3}He reaction was used to produce quasi monoenergetic neutrons between 8 and 14.5 MeV. Deuteron beams in the energy range between 5.3 and 11.9 MeV were provided by the Triangle Universities Nuclear Laboratory's (TUNL) tandem accelerator. Typical deuteron beam currents on target were 2 μA. The target consisted of a 3 cm long and 1 cm diameter cylindrical gas cell made of thin-walled stainless steel and filled with high-purity deuterium gas. A Havar foil of 6.35 μm thickness provided the seal to the accelerator vacuum. A 0.275 mm thick disk of tantalum served as beam stop. A schematic of the experimental setup is shown in Fig. 2. Depending on incident deuteron energy, the deuterium gas pressure was adjusted between 3 atm at the lowest energy and 4.6 atm at the highest energy to provide the desired neutron energy spread in the energy range investigated. Typically, the neutron energy spread was ± 120 keV at 0°. The uncertainty in the neutron energy scale is estimated to be ± 30 keV.

High-purity natural tantalum squares of 10 mm x 10 mm area and 0.125 mm thickness were attached to a low-mass holder and positioned 2.5 cm from the end of the deuterium gas cell at 0° relative to the incident deuteron beam direction (see Fig. 2). Due

to the kinematics and the cross section of the $^{2}H(d,n)^{3}He$ reaction, this finite geometry decreases the nominal neutron energy and increases its energy spread. Using the cross section of Refs. [3, 4] the effective mean neutron energy and its energy spread were calculated via Monte-Carlo simulation. Numerical values are given in Table I. Depending on incident neutron energy, the tantalum squares were irradiated over a period of 6 to 12 hours with constant neutron flux of 4.4 x 10^{6} to 2.9 x 10^{7} s^{-1}. A 1.5 inch diameter x 1.5 inch long cylindrical BC501A [5] neutron detector placed 3 m downstream of the deuterium gas cell served as on-line neutron flux monitor. Simple reaction kinematics shows that lower energy neutrons from the deuteron break-up process on structural materials of the deuterium gas cell can initiate the $^{181}Ta(n,2n)^{180g}$ reaction, if the incident deuteron energy is above about 9.8 MeV. This energy corresponds to neutron energies of above 12.5 MeV for the $^{2}H(d,n)^{3}He$ reaction, once the energy loss in the Havar foil is taken into account. Here, the breakup can take place on the entrance collimator (made of tantalum) of the deuterium gas cell, the Havar foil, and the tantalum beam stop. As a result, the contribution from the neutron continuum of the $^{2}H(d,np)X$ breakup channel (here X stands for heavy elements) has to be considered for our three highest neutron energies of 12.9, 13.9, and 14.39 MeV. However, this effect is small and corrections were applied [6,7]. In addition, measurements were performed with an empty gas cell at E_n=13 and 14.5 MeV. Here, the corrections were found to be about 2% and 5%, respectively. Neutrons from the deuteron breakup on the deuterium gas have energies below the $^{181}Ta(n,2n)^{180g}Ta$ threshold, and therefore, do not contribute in the deuteron energy range used in the present work.

As an additional cross check of the procedure used above E_n=12.5 MeV, the reaction $^{3}H(d,n)^{4}He$ was employed to produce 14.8 MeV neutrons. Here, a 2 Ci tritiated titanium target (see Ref. 8) was used to take advantage of the large cross section at about 100 keV incident deuteron energy. For this purpose, a 2 MeV deuteron beam from the tandem accelerator was energy degraded by a 6.35 μm Havar foil. In addition, the helium gas pressure (about 1.5 atm) in a small buffer cell located upstream of the tritiated target foil was fine-tuned to maximize the neutron yield.

The neutron fluence determination was accomplished by placing a gold (typically 44.6 mg) and an aluminum foil (typically 7.7 mg), each 10 mm x 10 mm in area and

0.025 mm in thickness, immediately downstream of the tantalum target foil (typically 0.225 g). The neutron activation cross sections for the reactions ^{197}Au($n,2n$)^{196}Au and ^{27}Al(n,α)^{24}Na were obtained from Ref. [9,10]. The threshold energy of the reaction ^{197}Au($n,2n$)^{196}Au is only about 450 keV higher than that of ^{181}Ta($n,2n$)^{180g}Ta. In addition, the ^{196}Au half-life time of $T_{1/2}$=6.17 d and its deexcitation γ-ray energy of 355.7 keV with I_γ=0.87 are very convenient features. As a result, the reaction ^{197}Au($n,2n$)^{196}Au provides for an excellent absolute neutron fluence determination for the present work. The reaction ^{27}Al(n,α)^{24}Na was used for E_n<12 MeV only. In this energy regime, the fluence determined from the ^{197}Au($n,2n$)^{196}Au and ^{27}Al(n,α)^{24}Na reactions agreed within uncertainties, after small corrections were applied for low-energy neutrons in the latter case. Because of its threshold energy of 3.2 MeV, the ^{27}Al(n,α)^{24}Na reaction is sensitive to breakup and room-return neutrons. Those effects have been studied and quantified in Refs. [11, 12].

After irradiation, the Ta/Au/Al sample stack was placed at a distance of 5 cm in front of a 20% High-Purity Germanium (HPGe) detector with the Ta foil facing the detector. This detector, located in TUNL's low-background counting facility, was well shielded against room and cosmic-ray background radiation. The efficiency and energy calibration of the detector were performed with the standard and well characterized radioactive sources ^{56}Co, ^{60}Co, ^{133}Ba, ^{137}Cs and ^{152}Eu. The half-life time of ^{180g}Ta is 8.154 h. The 93.4 keV γ-ray line originating from the electron capture (86%) to ^{180}Hf with I_γ=0.0451 was used in the analysis. The 103.6 keV γ-ray line from the beta decay (14%) to ^{180}W with I_γ=0.0081 was not used because of its larger statistical and branching uncertainties. A typical γ-ray spectrum is shown in Fig. 3. In addition to the three γ-ray lines at 93.4 keV, 103.6 keV, and 355.7 keV, the 1368.6 keV line from ^{24}Na is also indicated in Fig. 3. Background measurements with non-activated Ta/Au/Al foils were performed to account for the environmental background line at E_γ=92.4 keV, which originates from the β decay of ^{234}Th. After correcting for self-absorption in the Ta foil and coincidence summing (which turned out to be very small), decay curves were obtained, indicating good agreement between the measured and literature value for $T_{1/2}$.

For the Au and Al foils, corrections were applied for γ-ray attenuation in the Ta foil, ranging from 1.05% to 1.01 %, respectively.

The cross section of interest was obtained from the activation formula

$$A=\sigma\phi n(1-e^{-\lambda t_i})e^{-\lambda t_d}(1-e^{-\lambda t_c}),$$

where A is the number of decays per second, σ is the cross section in cm^2, ϕ is the incident neutron flux in $n.cm^{-2}.s^{-1}$, n is the number of target nuclei, t_i is the irradiation time, t_d is the decay time before the begin of the off-line γ-ray counting, t_c is the counting time, and finally λ is the decay constant.

III. RESULTS AND DISCUSSION

Figure 4 shows the measured cross-section data (upside-down triangles) between 7.9 MeV and 14.8 MeV in comparison to the data of Frehaut *et al*. [13] (solid pentagons), and some of the data [14-33] between 12 and 14.8 MeV already shown in Fig. 1. Our data are in striking disagreement with the former data set, which has been the most complete data set available for the reaction ^{181}Ta(*n,2n*)^{180g}Ta before the present data were obtained. However, in the 12 to 14.8 MeV energy range, our data are in excellent agreement with the majority of the data belonging to the lower band shown in Fig. 1. It should be noted that the disagreement with the data of Frehaut *et al*. [13] found in the present work is especially troublesome in view of Ref. [34], which states that the cross-section values reported by Frehaut *et al*. [13] were in fact too low by about 10%. As a result, the recent evaluation by Pereslavtsev and Fischer [35] overestimates the ^{181}Ta(*n,2n*)^{180g}Ta cross section at 14 MeV by about 80% compared to our work.

As can be seen in Fig. 4, the present data are in stark disagreement with the ENDF VII.1 [1] and TENDL [2] evaluations, which favor the upper band. Our data below 9 MeV were deconvoluted to correct for the strong energy dependence of the measured data.

Tables I and II present the cross-section results and the error budget, respectively. As shown in Table II, the overall uncertainty is governed by the sizeable uncertainty in the branching value I_γ for the 93.4 keV transition.

IV. TALYS CALCULATIONS

Figure 5 shows a TALYS calculation [36] with parameters adjusted to reproduce the present data. After fine-tuning the parameters of the various reaction models, TALYS generates cross-section results for all open reaction channels, including the (*n,2n*) channel to the isomeric state as well as to the ground state of ^{180}Ta. The default optical-model potentials were used to calculate the reaction cross sections and the total cross section. Moreover, TALYS yields the transmission coefficients for compound nucleus calculations and all cross sections and angular distributions for discrete states. The reaction mechanism, compound or direct, is calculated based on the Hauser-Feshbach formalism including width fluctuation corrections, which account for the correlation between the incident and outgoing waves. Because the projectile energy is above the particle-emission threshold of competing open channels, the width fluctuation correction factor is negligible in all methods implemented in TALYS, and the simple Hauser-Feshbach model is adequate to describe the compound-nucleus decay. The nuclear level density was fitted to properly reproduce the known *s*-wave resonance spacing (D_0 = 1.2 eV) at the neutron capture energy and also to reproduce the cumulative numbers of known low-lying states. The new energy-, spin- and parity-dependent nuclear level densities based on the microscopic combinatorial [37] provide the best fit to the experimental data (see solid curve in Fig. 5). The other level-density models like back-shifted Fermi gas, constant temperature, and generalized super-fluid models, predict larger (*n,2n*) cross-section values below 10 MeV.

As a by-product, for incident neutron energies of 13 MeV and above, cross-section data for the reactions ^{181}Ta(*n,p*)^{181g}Hf and ^{181}Ta(*n,d*)^{180m}Hf were obtained in the present work. These data are in good agreement with the present TALYS calculations, as can be seen in Fig. 6. The (*n,p*) data also agree reasonably well with the data of Ref. [14]. It is interesting to point out that the (*n,p*) and (*n,d*) cross-section data of ^{181g}Ta are 300 and 6000, respectively, smaller than the (*n,2n*) reaction cross section.

The neutron induced cross sections on ^{181}Ta are also important for NIF diagnostic and can be used for determining the areal density of the deuterium-tritium fuel. These reactions, as shown in Fig. 6, have different threshold and can sample different part of the

NIF spectrum. For example, the (n,γ) cross section is most sensitive to neutrons below 1 MeV and the cross section increases as the neutron energy decreases. On the other hand, the ($n,2n$) reaction is dominated by the 14.1 MeV neutrons. By measuring the ratio of the concentrations of these two radioactive products (i.e., ^{182}Ta/^{180}Ta) one can determine the average energy of the down scattered neutrons and correlate this to the areal density of the cold fuel. In addition, the newly obtained cross sections for (n,p) and (n,d) reactions, can also be used to further constrain the shape of the NIF spectrum.

It is of special interest to study the reaction cross section to the isomeric state (J^{π} = 9^{-}) of ^{180}Ta after the statistical-model calculations to the ground state were constrained. The half-life time of the isomeric state is $T_{1/2} \geq 10^{15}$ years, and measuring the ^{181}Ta($n,2n$)^{180m}Ta reaction cross section leading to this state remains an experimental challenge. Because of the large spin difference between the isomeric and ground state (ΔJ = 8), and the absence of levels located below the isomeric state with adjacent spin values, ^{180m}Ta is a classical example of a "spin-trap" isomer. The calculated cross section for the reaction ^{181}Ta($n,2n$)^{180m}Ta is shown in Fig. 5 (dotted curve) in comparison to the ground-state cross section and its associated evaluations. Despite the large spin difference between the isomeric and the ground state, the isomeric cross-section ratio ^{180m}Ta/^{180g}Ta, for example at 14.5 MeV, is 44% as shown in Fig. 7. According to our knowledge, this is the largest isomeric ratio observed for any ($n,2n$) reaction with spin difference of ΔJ = 8.

V. CONCLUSIONS

We propose to adopt the present TALYS calculations in the 10 to 15 MeV energy range as the new recommended evaluations for the ^{181}Ta($n,2n$)^{180g}Ta and ^{181}Ta($n,2n$)^{180m}Ta cross section. Below 10 MeV the present data are lower in magnitude than the TALYS calculations. An unexpectedly large cross section is predicted by the TALYS calculations for the ($n,2n$) reaction to the ^{180m}Ta isomeric state.

ACKNOWLEDGMENTS

The authors acknowledge valuable contributions from M. Bhike, S.W. Finch, C.R. Howell, J.H. Kelley, J.B. Wilhelmy and D.J. Vieira. Fruitful discussions with S. Goriely

are gratefully acknowledged. We would like to thank C. Cerjan (LLNL) for modeling of NIF neutron spectrum. This work was supported in part by the National Nuclear Security Administration under the Stewardship Science Academic Alliance Program through the US Department of Energy Grant No. DE-FG52-09NA29465. This work was performed under the auspices of the U.S. Department of Energy by Lawrence Livermore National Laboratory under Contract DE-AC52-07NA27344.

References

[1] M. B. Chadwick, M. Herman, P. Oblozinsky, *et al.*, Nucl. Data Sheets **112**, 2887 (2011).
[2] http://www.talys.eu/tendl/.
[3] H. Liskien and A. Paulsen, Nuclear Data Tables **11**, 569 (1973).
[4] M. Drosg, http://homepage.univie.ac.at/manfred.drosg/drosg2000.html.
[5] D. E. Gonzalez Trotter, F. Salinas Meneses, W. Tornow, *et al.*, Nucl. Instrum. Methods in Phys. Res. **599**, 234 (2009); http://www.detectors.saint-gobain.com/.
[6] R. Raut *et al.*, Phys. Rev. C **83**, 044621 (2011).
[7] A.P. Tonchev *et al.*, Phys. Rev. C **77**, 054610 (2008).
[8] C. Bhatia, S.W. Finch, M.E. Gooden, W. Tornow, submitted to Phys. Rev. C
[9] K.I. Zolotarev, INDC (NDS)-0526 (2008).
[10] K.I. Zolotarev, INDC (NDS)-0546 (2009).
[11] Y.Kasugai *et al.*, Ann. Nucl. Energy **25**, 23 (1998).
[12] C. Bhatia *et al.*, to be submitted to Nucl. Instrum. Methods in Phys. Res.
[13] J. Frehaut, A. Bertin, R. Bois, J. Jary, Int. Symp. on Neutron Cross Sections from 10 to 50 MeV, Upton, LI, USA, p.399 (1980).
[14] J. Luo, F. Tuo, and X. Kong, Phys. Rev. C 79, 057603 (2009).
[15] A.A. Filatenkov and S.V.Chuvaev, Khlopin Radiev. Inst., Leningrad Reports, No. 258 (2001).
[16] A.A. Filatenkov *et al.*, Khlopin Radiev. Inst., Leningrad Reports, No. 252 (1999).
[17] Y. Kasugai, *et al.*, JAERI-M Reports, No.93, 046, p.277 (1992).
[18] A. Takahashi *et al.*, Osaka Univ., OKTAVIAN Reports, No.92, p.01 (1992).
[19] F. Peiguo *et al.*, Chinese J. of Nuclear Physics (Beijing) **7**, 242 (1985).
[20] L. Hanlin, Z. Wenrong and Fan Peiguo, Nucl. Sci. Eng. **90**, 304 (1985).
[21] J. Csikai, in Proc. of the Int. Conf. on nuclear Data for Science and Technology, Antwerpen, p.414 (1982).

[22] T.B. Ryves and P. Kolkowski, *Journ. of Phys. G, Nucl. and Part. Phys*. 6, 771 (1980).
[23] S.C. Misra and U. C. Gupta, *Journ. of Phys. G, Nucl. and Part. Phys.* **5**, 855 (1979).
[24] N. Lakshmana Das *et al.,* Nuovo Cimento A, **48**, 500 (1978).
[25] L.R. Veeser, E.D. Arthur and P.G. Young Phys. Rev. C **16**, 1792 (1977).
[26] T. Akiyoshi *et al.,* Journal of Nucl. Sci. and Technology **11**, 523 (1974).
[27] R. Mogharrab and H. Neuert, Atomkernenergie, **19**, 107 (1972).
[28] M. Bormann *et al.,* Nucl. Phys. A **115**, 309 (1968).
[29] R.J. Prestwood and B.P. Bayhurst , Phys. Rev. **121**, 1438 (1961)
[30] A. Poularikas *et al.,* Journal of Inorganic and Nuclear Chemistry **13**, 196 (1960).
[31] V.J. Ashby *et al.,* Phys. Rev. **111**, 616 (1958).
[32] L. Rosen and L. Stewart, Phys. Rev. **107**, 824 (1957).
[33] E.B. Paul and R.L. Clarke, Canadian Journal of Physics **31**, 267 (1953).
[34] H. Vonach, A. Pavlik, B. Strohmaier, Nucl. Sci. Eng. **106**, 409 (1990).
[35] P. Pereslavtsev and U. Fischer, Nucl. Instr. and Meth. in Phys. Res. B **248**, 225 (2006).
[36] A. Koning, S. Hillaire, and M.C. Duijvestijn, AIP Conf. Proc. **769**, 1154 (2005).
[37] S. Goriely, S. Hilaire, A. J. Koning, Phys. Rev. C **78**, 064307 (2008).

TABLE I. Summary of cross-section results for the reaction ^{181}Ta(n,$2n$)^{180g}Ta.

E_n (MeV)	$\pm\Delta E_n$	^{181}Ta(n, $2n$)^{180g}Ta		
		σ (mb)	$\Delta\sigma_1$	$\Delta\sigma_2$
7.93	0.20	27.06	0.40	1.36
8.18	0.19	97.44	0.84	4.51
8.43	0.19	154.40	1.10	7.20
8.93	0.20	404.61	1.30	21.59
9.43	0.20	723.28	2.90	33.60
9.91	0.24	862.74	3.20	46.05
10.91	0.23	1123.37	4.22	62.32
11.90	0.22	1206.11	5.45	55.85
12.90	0.22	1293.53	6.66	67.40
13.90	0.22	1189.25	7.95	61.56
14.39	0.22	1232.25	10.02	63.07
14.80	0.05	1233.70	11.56	60.57

ΔE_n = Neutron energy spread as explained in the text.
$\Delta\sigma_1$ = Statistical uncertainty
$\Delta\sigma_2$ = Total uncertainty

TABLE II. Sources and approximate magnitudes of the uncertainties (in%) in the present cross-section measurement.

Uncertainty	**Magnitude (%)**
Statistics	1–1.5
Sample mass	<1
Detector efficiency	2–3
Branching ratio	3.5
Product half-life	≤ 0.5
Monitor cross section	1–2 (Al) 1–3 (Au)
Low-energy neutrons	<1
Total*	4.4–5.9

* Total uncertainty obtained from individual uncertainties added in quadrature.

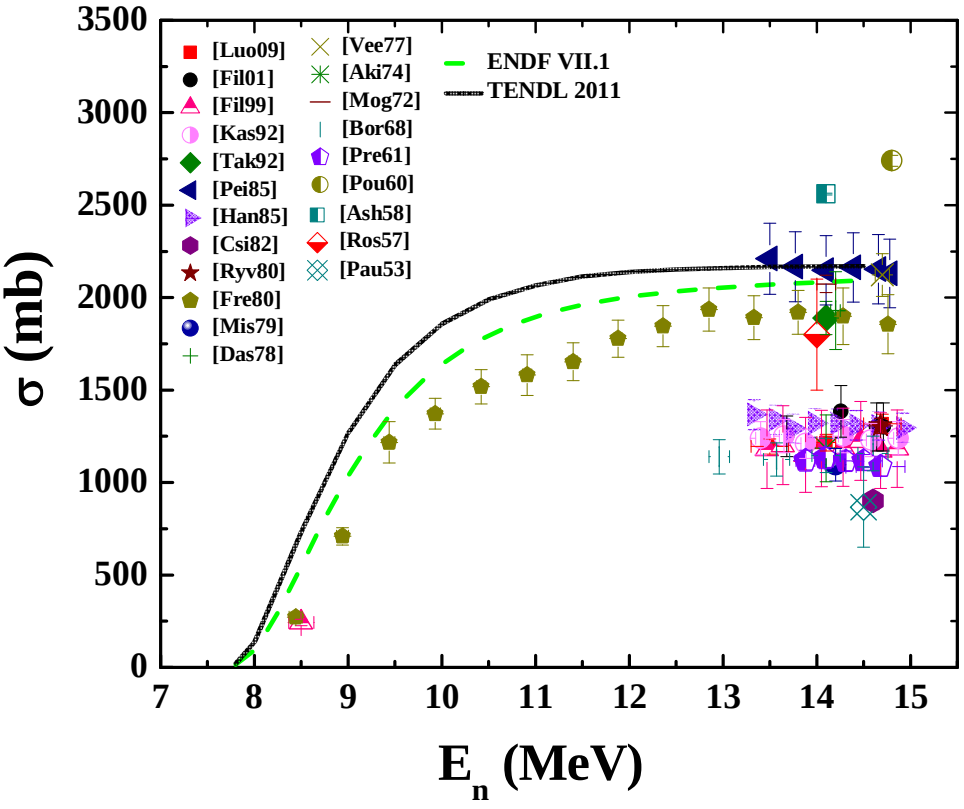

FIG. 1. Existing angle-integrated cross-section data for the ^{181}Ta(*n*, *2n*) ^{180g}Ta reaction [13-33] in comparison to the ENDF VII.1 [1] and TENDL 2011 [2] evaluations.

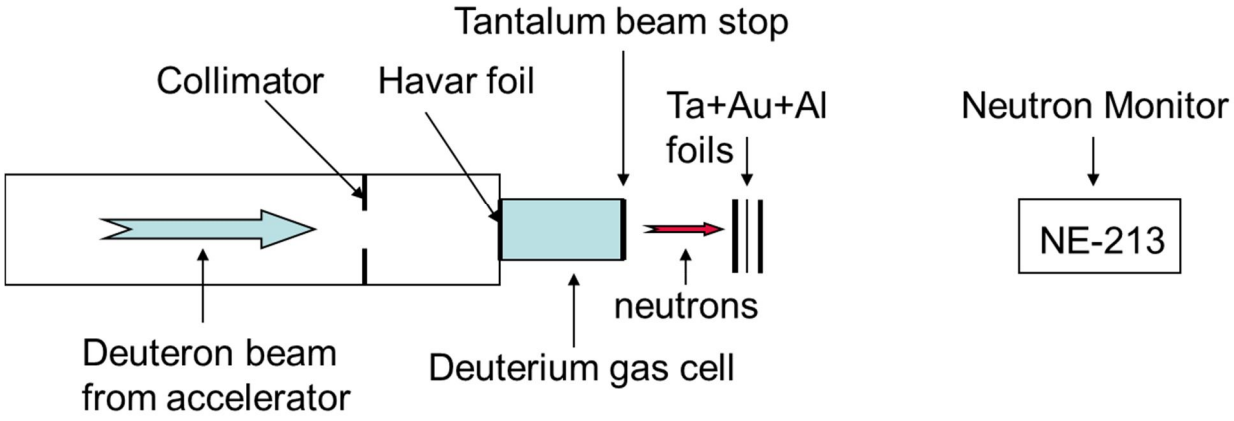

FIG. 2. (Color online) Schematic of experimental setup used for neutron activation measurements, consisting of deuterium gas cell for $^{2}H(d,n)^{3}He$ reaction, Ta, Au and Al targets, and neutron monitor.

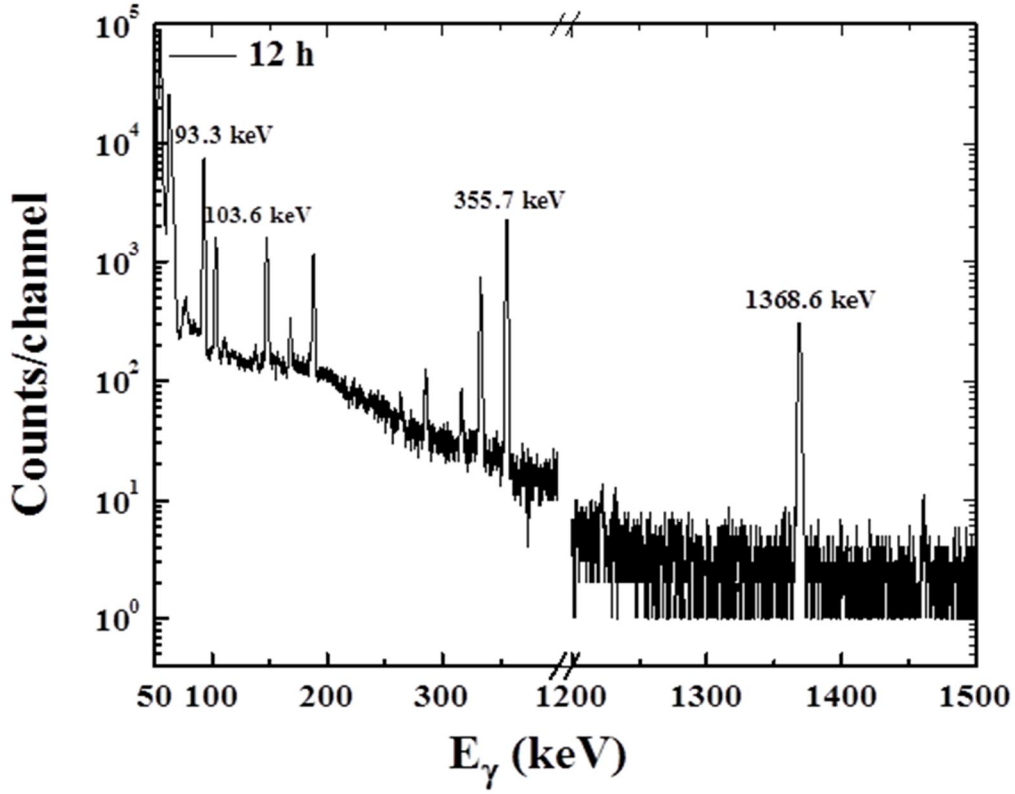

FIG. 3. Partial gamma-ray spectrum of ^{180g}Ta obtained with a 20% efficient HPGe detector and recorded after twelve hours of neutron activation of ^{181}Ta at E_n = 14.39 MeV. The lines of interest are labeled.

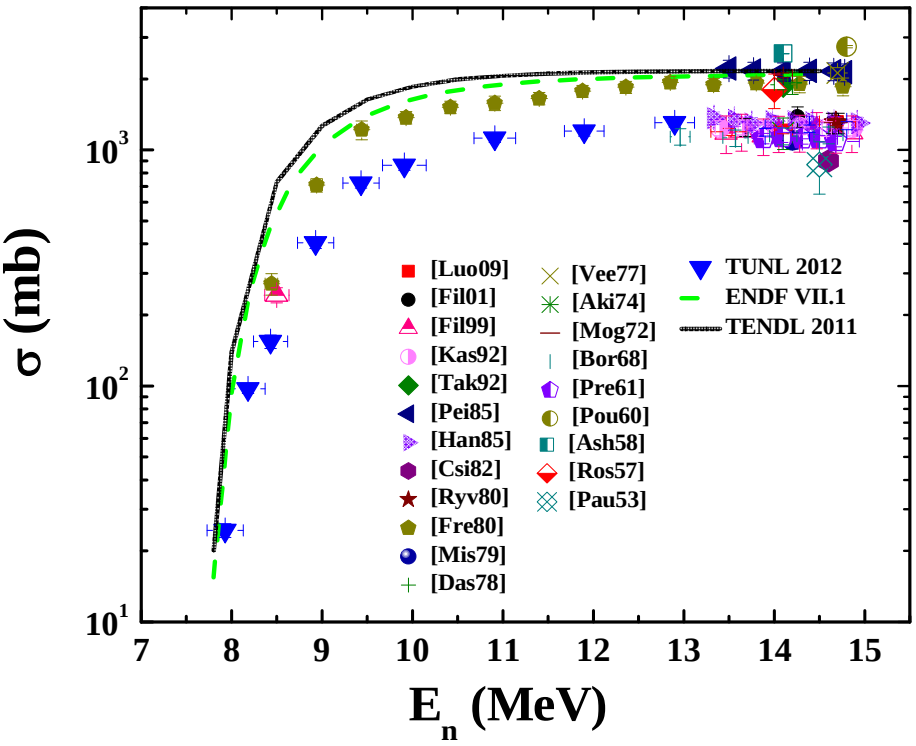

FIG. 4. The present cross-section results obtained for the ^{181}Ta(n,$2n$)^{180g}Ta reaction is shown by the up-side-down triangles in comparison to previous measurements and recent evaluations.

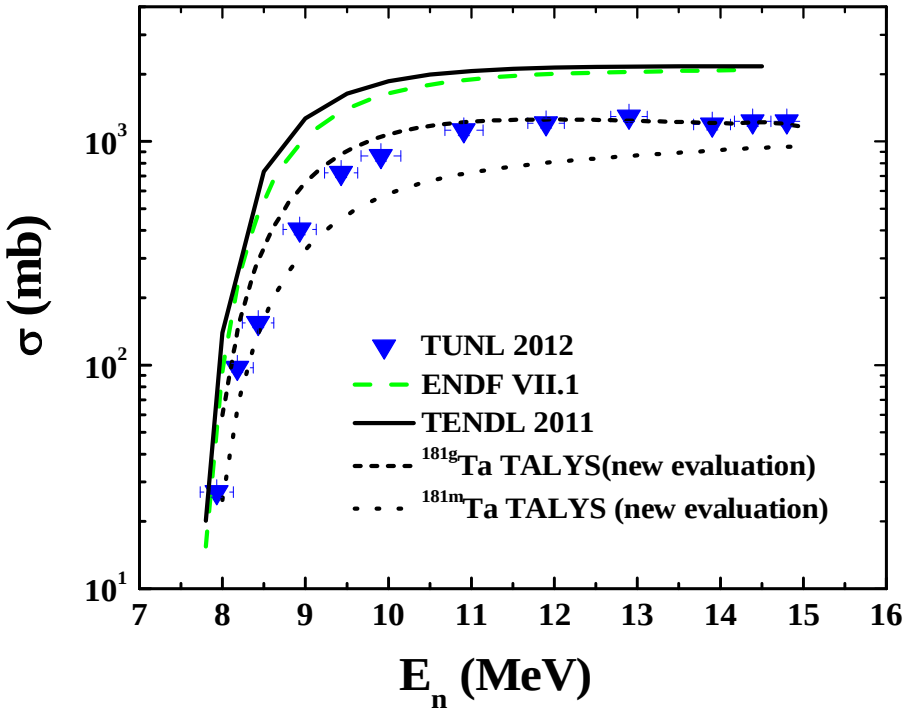

FIG. 5: (Color online) TALYS calculations [36] (short dashed and dotted curves) with parameters adjusted to reproduce the present data, in comparison to the ENDF VII.1 [1] and TENDL 2011 [2] evaluations.

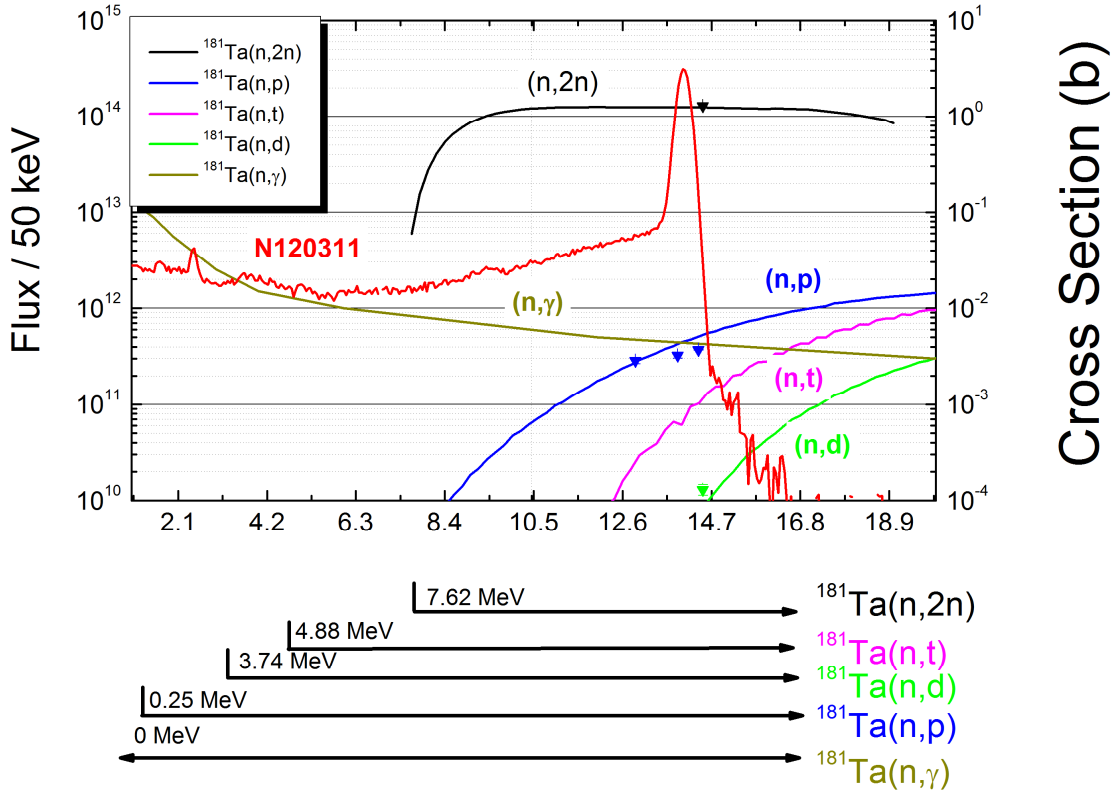

FIG. 6. (Color online) Present cross-section data for ^{181}Ta(n,2n)^{180g}Ta, ^{181}Ta(n,p)^{181g}Hf , ^{181}Ta(n,t)^{179}Hf, ^{181}Ta(n,d)^{180m}Hf and ^{181}Ta(n,γ)^{182}Ta reactions in comparison to TALYS [36] calculations.

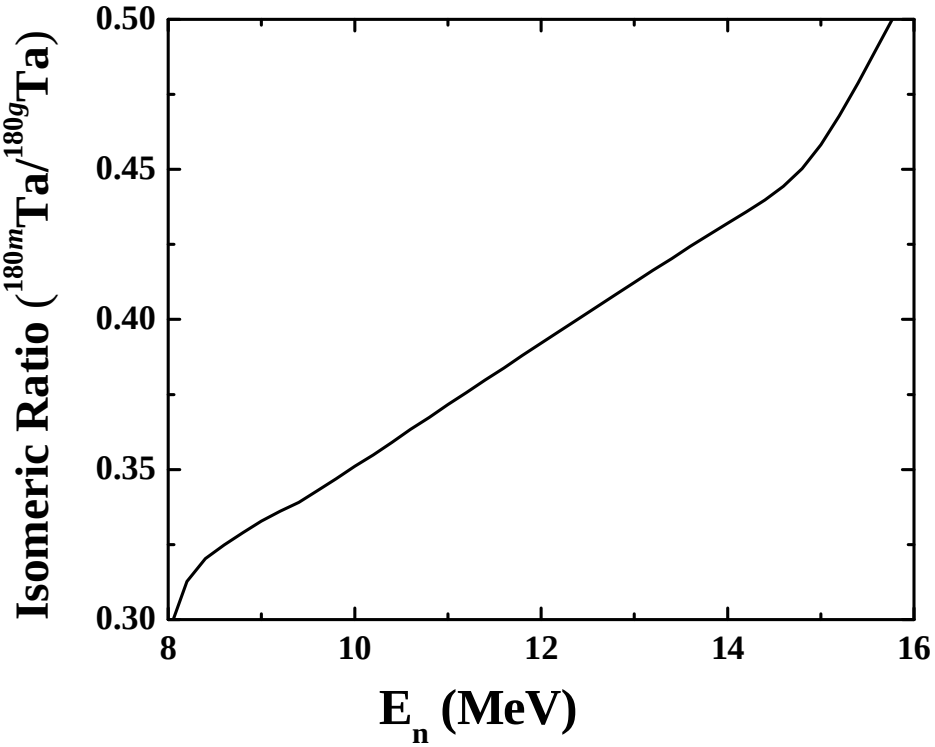

FIG. 7. Isomeric cross-section ratio ^{180m}Ta/^{180g}Ta calculated using TALYS [36].